RESEARCH PAPER

A novel smartphone-based electrochemical cell sensor for evaluating the toxicity of heavy metal ions Cd^{2+}, Hg^{2+}, and Pb^{2+} in rice

Donglei Jiang [1] · Kaikai Sheng [1] · Guoyue Gui [1] · Hui Jiang [2] · Xinmei Liu [2] · Lifeng Wang [1]

Abstract

A novel smartphone-based electrochemical cell sensor was developed to evaluate the toxicity of heavy metal ions, such as cadmium (Cd^{2+}), lead (Pb^{2+}), and mercury (Hg^{2+}) ions on Hep G2 cells. The cell sensor was fabricated with reduced graphene oxide (RGO)/molybdenum sulfide (MoS_2) composites to greatly improve the biological adaptability and amplify the electrochemical signals. Differential pulse voltammetry (DPV) was employed to measure the electrical signals induced by the toxicity of heavy metal ions. The results showed that Cd^{2+}, Hg^{2+}, and Pb^{2+} significantly reduced the viability of Hep G2 cells in a dose-dependent manner. The IC_{50} values obtained by this method were 49.83, 36.94, and 733.90 μM, respectively. A synergistic effect was observed between Cd^{2+} and Pb^{2+} and between Hg^{2+} and Pb^{2+}, and an antagonistic effect was observed between Cd^{2+} and Hg^{2+}, and an antagonistic effect at low doses and an additive effect at high doses were found in the ternary mixtures of Cd^{2+}, Hg^{2+}, and Pb^{2+}. These electrochemical results were confirmed via MTT assay, SEM and TEM observation, and flow cytometry. Therefore, this new electrochemical cell sensor provided a more convenient, sensitive, and flexible toxicity assessment strategy than traditional cytotoxicity assessment methods.

Keywords Cell-based sensor · Heavy metal ion toxicity · Smartphone · Electrochemical evaluation

Introduction

Heavy metals are metals with a specific gravity greater than five that include gold, silver, copper, iron, mercury, lead, and cadmium [1]. These heavy metals accumulate in the human body to a certain degree, cause chronic or acute poisoning, and place serious threats on human health. Long-term intake of trace amounts of heavy metal food will cause accumulative poisoning, which can lead to human immune system dysfunction [2]. Cadmium, lead, mercury, and their compounds in foods can seriously damage the nervous system of the human body and have certain carcinogenic, teratogenic, and mutagenic effects on the human body [3]. At present, there are several methods for heavy metal ion analysis including atomic absorption spectrometry, atomic fluorescence spectrometry, and inductively coupled plasma mass spectrometry [4–7]. These methods are widely used due to their advantages such as high sensitivity, good selectivity, and less interference, but they all require tedious sample pretreatment, time-consuming operation, and high costs, and cannot be used for on-site detection [8]. Therefore, it is necessary to develop a fast, sensitive, low-cost, and portable detection method to replace the more complex conventional methods. While biosensing technology mimics an in vivo environment, the sensitive detection of heavy metal concentrations and the real evaluation of its toxicity can be easily realized through the conversion between biological recognition and electrical signaling [9]. Cell sensors are a hot topic in biosensor research. They utilize living cells as sensitive components to detect functional information of cells or properties of harmful targets by measuring biochemical signal transformation [10–12]. Thus, the cell sensor can be used to analyze various trace heavy metal samples without changing the identification elements, and it has incomparable advantages such as wide detection range, low demand for instrumentation, and convenient operation.

✉ Lifeng Wang
  wanglifeng_8@163.com

1 College of Food Science and Engineering/Collaborative Innovation Center for Modern Grain Circulation and Safety/Key Laboratory of Grains and Oils Quality Control and Processing, Nanjing University of Finance and Economics, Nanjing 210023, Jiangsu, China

2 Nanjing Institute for Food and Drug Control, Nanjing 211198, Jiangsu, China

This study introduces a portable electrochemical cell sensor based on a smartphone for the effective detection and toxicity evaluation of heavy metal ions. Portable electrochemical detection devices employed in the analysis convert the biochemical responses of cell sensors into electrochemical signals that can be rapidly analyzed [13–15]. As a convenient multifunctional mobile device in modern life, smartphones also have unique advantages as sensing platforms [16–18]. Usually, it can be employed as the core center of operation control and data processing. Then, electrochemical workstations can be controlled by the smartphone through the USB wired connection mode or wireless connection modes such as Bluetooth™ or WiFi, which can achieve the purpose of real-time detection of targeted heavy metals and greatly improve the detection efficiency, reduce the equipment cost, and save valuable time [19–21]. To improve the stability and repeatability of the sensor, a screen-printed carbon electrode (SPCE) was used instead of the traditional three electrodes, which can significantly reduce the detection cost and relieve the workload [22]. Based on the exploration of low-cost disposable electrodes, modification of electrodes with highly conductive and biocompatible nanomaterial is an important part of biosensor design.

Molybdenum disulfide (MoS_2) is a kind of two-dimensional layered semiconductor material with very stable structure and excellent biological properties [23–25]. However, MoS_2 has poor conductivity and can easily aggregate, so it is usually combined with other conductive materials. Therefore, graphene oxide (GO), which has a similar structure with MoS_2 and strong electrical conductivity, has been considered a versatile scaffold for the synthesis of hybrid nanocomposite with improved properties [26–28]. Due to the electrostatic interaction, the molybdate group of MoS_2 will be firmly adsorbed to the GO surface. Meanwhile, the GO gradually loses its oxygen-containing group and is reduced to RGO, forming a dense structure. The RGO/MoS_2 composite material can further improve the electrical conductivity of the electrode surface, enhance the sensitivity of the sensor, and provide a stable environment for cell growth.

Folic acid (FA), as an important B vitamin with nontoxic, stable, and low immunogenicity [29], has high affinity (Kd of 0.1–1 nM) to its specific target folate receptor (FR) which is a folate-binding protein with a naturally 38-kDa glycol-polypeptide [30]. FR is known to be overexpressed by many human cancer cells (up to 100–300 times higher than normal cell), including malignancies of the liver, ovary, lung, kidney, testis, and prostate, but rarely expressed in normal tissue [31]. Hep G2 cells were derived from the tumor tissue of a 15-year-old Argentine boy with well-differentiated hepatocellular carcinoma in 1975. There were high-expression FR on the surface of Hep G2 cells [32]. Therefore, Hep G2 cells can be precisely immobilized on the SPCE through the high-affinity binding between FR and FA, thus enabling the rapid and efficient preparation of cell sensors.

We propose a novel and convenient portable electrochemical cell sensor based on a smartphone, where the toxic effect of heavy metal ions on the Hep G2 cells was evaluated by electrochemical differential pulse voltammetry (DPV) analysis. Conventional cytotoxicity experiments such as MTT and flow cytometry have been compared with electrochemical sensing methods. The analytical results are similar to those of electrochemical analysis, which verify the accuracy and effectiveness of the developed electrochemical cell sensing method for heavy metal ion evaluation. At the same time, the relationship between the toxicity of heavy metal ions and the mechanism of cell apoptosis was discussed through electrochemical data analysis. Therefore, this study demonstrated a simple and convenient cell sensing method, which provides a new choice for the evaluation of heavy metal ions toxicity.

Materials and methods

Materials and apparatus

Hep G2 human liver cancer cells were obtained from the cell bank of the Chinese Academy of Sciences (Shanghai, China). Thioacetamide (CH_3CSNH_2), ammonium sulfate hydrate (($NH_4)_6Mo_7O_{24} \cdot 4H_2O$), folic acid ($C_{19}H_{19}N_7O_6$), dimethyl sulfoxide (DMSO), and thiazole blue tetrazole bromide (MTT) were purchased from Alighting Biochemical Technology Co., Ltd (Shanghai, China). Graphene oxide powder was obtained from Xianfeng nano co., Ltd. (Nanjing, China). 0.25% trypsin solution, dual antibody (penicillin-streptomycin), and all biological kits were obtained from Beyotime Biotechnology (Shanghai, China). DMEM medium and fetal bovine serum (FBS) were purchased from SenBeiJia Biological Technology Co., Ltd. (Nanjing, China). Mercury chloride, lead chloride, and cadmium chloride were purchased from Sinopharm Chemical Reagent Co., Ltd. (Shanghai, China), heavy metal ions were prepared with ultrapure salts, and different anions (chloride) were tested, and no significant toxicity to cells was found.

A XenSTAT (II) portable electrochemical workstation and SPEnsor screen-printing electrode were developed by Xenslet studio (Shanghai, China). The Android smartphone installed with homemade APP-xenSTAT undertakes the electrochemical data acquisition, analysis, storage andtransmission. S4800 scanning electron microscope (Hitachi, Japan), inverted fluorescence microscope (Olympus, Japan), X-ray diffractometer (XRD) (Philips X'pert MPD, Netherlands), and TENSOR 27 Fourier infrared spectrometer (BRUKER, Germany) were used for material characterization. A CL17R frozen high-speed centrifuge, CO_2 incubator (Thermo, USA), Spectra MAX 340 Microplate reader (Molecular Devices, USA),

and BD FACSVerse flow cytometry (BD instruments, USA) were used for sample analysis.

Preparation of RGO/MoS₂ composites

Sixty milligrams (optimization seen in the Supplementary Information (ESM)) of monolayer graphene oxide (GO) powder was uniformly dispersed in 10 mL deionized water, and the desired concentration of monolayer GO dispersion was obtained after ultrasonic treatment. RGO/MoS_2 composite was synthesized by the hydrothermal synthesis method, which is, in brief, the following: first, the GO dispersion was added to a mixture of 70.5 mg ammonium molybdate hydrate and 60.0 mg thioacetamide (the precursor of MoS_2), and then the mixed liquid was moved into a stainless steel high-temperature reactor equipped with polytetrafluoroethylene. After heating at 190 °C for 24 h, the composite material was obtained after being taken out and dried at room temperature. Then, an appropriate amount of the composite material was taken out and dispersed in pure water for later use.

Electrode modification and cell immobilization

A step-by-step modification process of the electrochemical cell sensor is illustrated in Scheme 1. To avoid interference, the bare screen-printed electrode was first scanned from −0.2 to 0.6 V by dropping 1 mM of $Fe(CN)_6^{3-/4-}$ electrolyte using cyclic voltammetry (CV) to remove the electrode surface oxides before electrode modification. Then, 10 mg FA was dispersed in 10 mL ultrapure water and mixed well. Ten microliters of the FA dispersion was mixed with 20 μL of the 0.7 mg/mL RGO/MoS_2 composite and dripped on the electrode surface, and the electrode was then dried with pure nitrogen at room temperature. The electrode was then washed with ultrapure water to remove the excess mixture. Immediately after cleaning, 20 μL of HepG2 cells suspension at a concentration of 2×10^6 cells/mL was dropped onto the electrode surface, and after incubation at 37 °C and 5% CO_2 for 30 mins, the electrode was immersed in pH 7.4 PBS buffer to remove uncaptured cells. Finally, the electrode was stored in an incubator at 37 °C and 5% CO_2 for later use.

Electrochemical measurements

After the 2×10^6 cells/mL of the Hep G2 cells were immobilized on the $RGO/MoS_2/FA$ modified electrode, after a short incubation, the serum-free DMEN culture medium containing different kinds and concentrations of heavy metal ions was added onto the electrode surface. Meanwhile, an electrochemical DPV method was used to monitor the electrochemical signal response of the Hep G2 cells stimulated by heavy metal ions. The appropriate concentrations (5 to 160 μM of Cd^{2+}, Hg^{2+}, and 10 to 3000 μM of Pb^{2+}) of the heavy metal ions were prepared using the composite buffer solution contained with NaCl, KCl, HEPES, $CaCl_2$, and glucose, and adjusted pH to 7.3. According to the different types of heavy metals, the cells were divided into three groups and the cells not exposed to heavy metal ions were used as controls. In addition, the cells on the modified electrodes were all
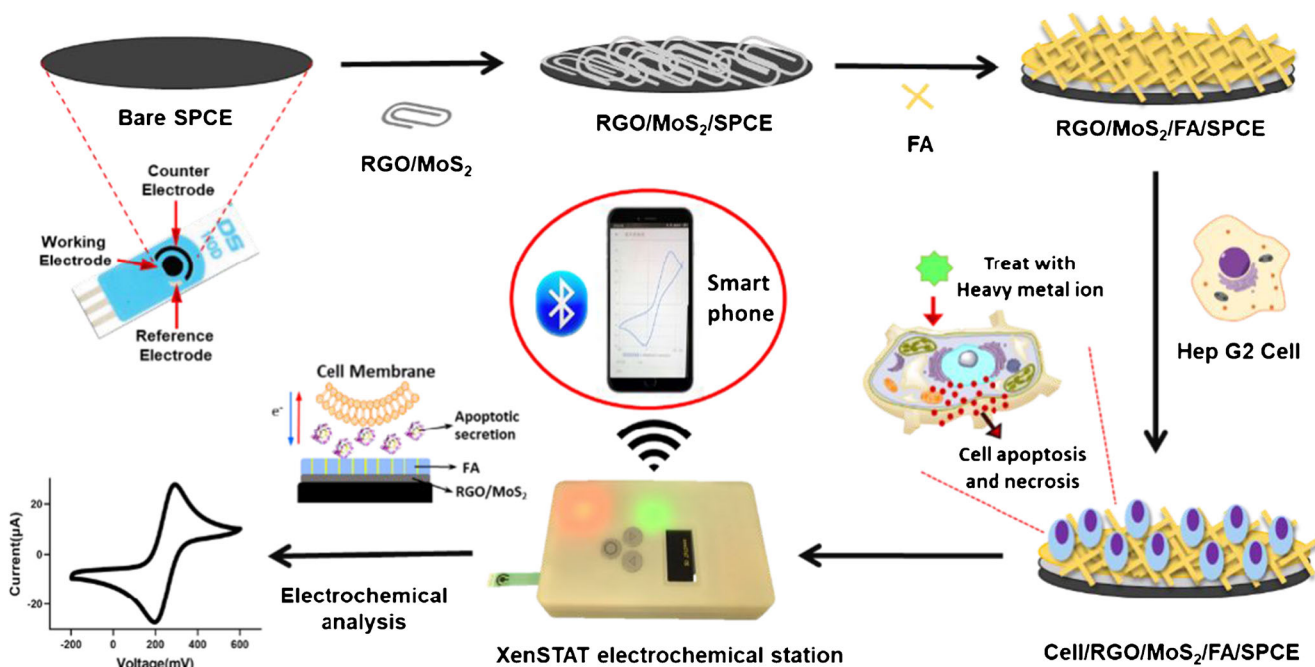
Scheme 1 Schematic diagram of the preparation and detection process of the smartphone-based electrochemical cell sensor

incubated with different concentrations of Cd^{2+}, Hg^{2+}, and Pb^{2+} for 6 h to analyze the individual and combined toxicity.

Electrochemical experiments were carried out on a portable electrochemical workstation with disposable SPCE (carbon working electrode, counter electrode, and silver chloride reference electrode, all were 3 mm diameter). Hep G2 cells immobilized on working electrode were used for biosensing evaluation. All electrochemical experiments were performed at room temperature. The cytotoxicities of heavy metal ions were calculated as follows [30]:

$$\text{Cytotoxicity } (\%) = 100 \times [(I_{metal} - I_{cell})/(I_{modified} - I_{cell})] \quad (1)$$

where I_{metal} is the peak current of the cell sensor treated with heavy metal ions measured by DPV method, I_{cell} is the peak current of the cell sensor without heavy metal ion stimulation measured by the DPV method, and $I_{modified}$ is the peak current of the RGO/MoS$_2$/FA modified electrode without the cell measured by DPV method. Detailed experimental parameters are as follows: cyclic voltammetry (CV) had a scan range of $-0.2\sim0.6$ V and scan rate of 0.1 V/s. Differential pulse voltammetry (DPV) had a scan range of $-0.2\sim0.6$ V and a pulse amplitude of 0.1 V.

Statistical analysis

All electrochemical measurements were repeated in triplicate. Data were expressed as mean ± SD. Statistical analysis was performed using SPSS 22.0 software. Student's t test was used to determine the significance of difference. $p<0.05$ was considered statistically significant between the control and the test groups.

Individual heavy metal ion toxicity dose-response relationships were biometrically modeled using the median-effect equation:

$$\frac{f_a}{f_u} = \left(\frac{D}{D_m}\right)^m \quad (2)$$

where D is the concentration, D_m is the concentration for the 50% effect, f_a is the fraction affected by concentration D, f_u is the unaffected fraction ($f_a = 1 - f_u$), and m is the sigmoid coefficient of the dose-response curve: where $m = 1$, $m > 1$, and $m < 1$ indicate hyperbolic, sigmoidal, and negative sigmoidal dose-response curves, respectively.

The combination index (CI) was used to analyze the combined toxicity of multiple heavy metal ions [33–35]. The results are calculated according to the following formula:

$$^n(CI)_x = \sum_{j=1}^n \frac{(D)_j}{(D_x)_j} \quad (3)$$

where $^n(CI)_x$ represents the combination index when $x\%$ inhibition rate was generated under the stimulation of n heavy metal ions. $(D)_j$ represents the concentration of $x\%$ inhibition under the combined stimulation of n heavy metal ions. $(D_x)_j$ indicates the concentration of $x\%$ inhibition under the single stimulation of n heavy metal ions, where $CI < 0.9$ indicates a synergetic effect, $CI = 0.9\sim1.1$ indicates an additive effect, and $CI > 1.1$ indicates antagonism. All CI values were calculated by CompuSyn software.

Results and discussion

Working principles of the cell-based sensor for heavy metal toxicity assessment

Scheme 1 illustrates the preparation process and working principle of the Hep G2 cell sensor for the determination and evaluation of the cytotoxicity of heavy metal ions. Hep G2 cells were successfully immobilized on the surface of RGO/MoS$_2$/FA modified SPCE. The RGO/MoS$_2$ composites were synthesized to improve the electrochemical conductivity and sensitivity of the cell sensor. Due to the electrostatic action, a molybdenum acid group was adsorbed firmly on the surface of graphene oxide. With the action of high temperature and high pressure, ammonium molybdate hydrate and thioacetamide reacted to form molybdenum disulfide. At the same time, GO gradually lost its oxygen-containing groups and was reduced to RGO, resulting in the formation of densified structure. The concentration of RGO/MoS$_2$ was optimized using an electrochemical test (shown in ESM Fig. S3). 0.7 mg/mL of RGO/MoS$_2$ was selected to modify the SPCE according to the optimization results. FA can specifically capture and immobilize cancer cells, and, therefore, it was combined with RGO/MoS$_2$ and dripped on the SPCE to improve cell adhesion and protect cells from external influences. When the Hep G2 cells were stimulated with heavy metal ions, due to the toxic effect of heavy metal ions, cell apoptosis and necrosis will be induced, which will decrease cell vitality and adhesion and then weaken the electrochemical signal of cells on SPCE. By determining the dose relationship between the concentration of heavy metal ions and the electrochemical signal strength of cells, the toxicity of heavy metal ions can be monitored and evaluated. In addition, through the cooperation of a portable electrochemical workstation and a smartphone, real-time determination of heavy metal toxicity in samples can be realized, which satisfies the demands of on-site evaluation.

Electrochemical characteristics of the cell-based sensors

In this study, CV and DPV methods were used to conduct electrochemical characterization of different modification phases of the cell sensor. As shown in Fig. 1 A and B, the
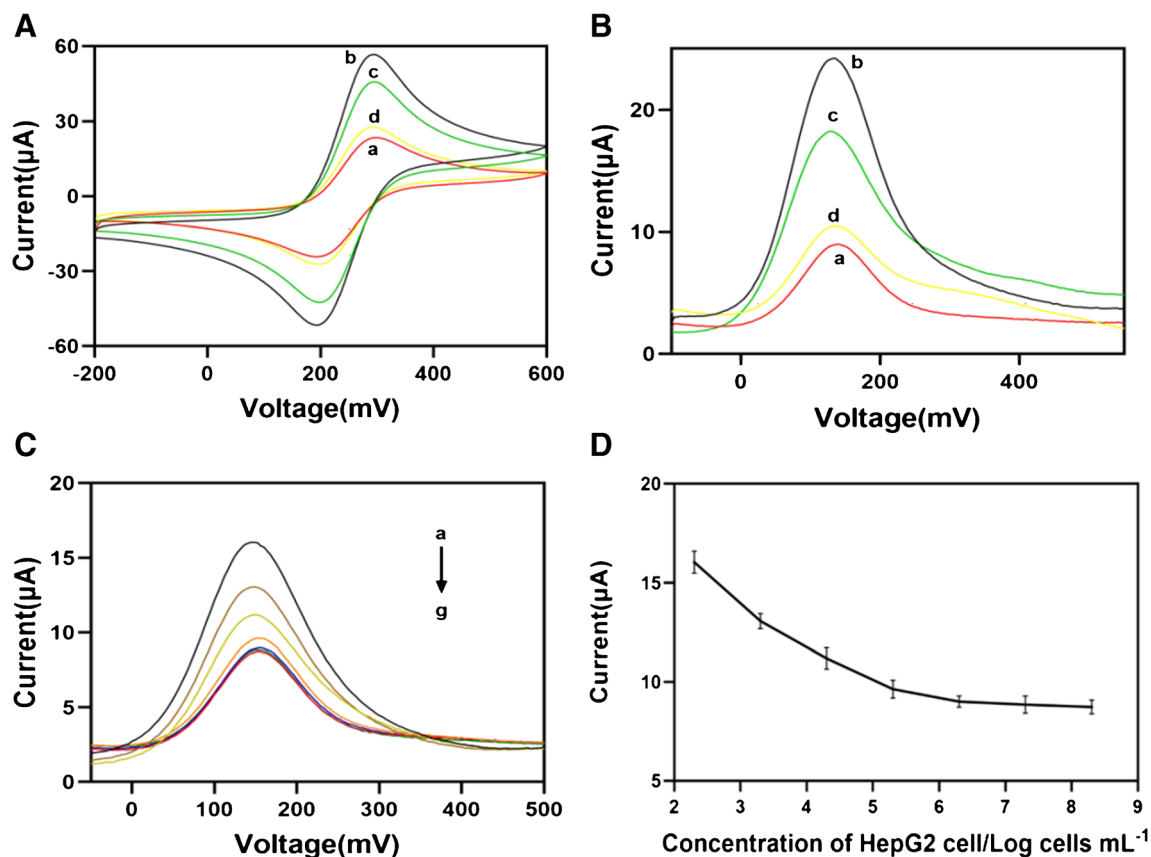
Fig. 1 Electrochemical characterization of the cell sensor. (A) Cyclic voltammetry and (B) differential pulse voltammetry of (a) Cell/FA/RGO/MoS$_2$/SPCE, (b) RGO/MoS$_2$/SPCE, (c) FA/RGO/MoS$_2$/SPCE, and (d) bare SPCE. (C) Differential pulse voltammograms of different cell numbers from a to g: 2×10^2 cells/mL to 2×10^8 cells/mL. (D) Linear regression curve between cell concentration and Ip value

bare electrode had a standard redox peak with a small peak current value of 10.46 μA (curve d), which proved that the electrode surface was clean and free of sundries and can be used for subsequent tests. Due to its good electrical conductivity, RGO can be used to amplify electrical signals and improve detection sensitivity. Therefore, when the electrode was modified with the RGO/MoS$_2$ composite, the peak current significantly increased to 24.17 μA (curve b), indicating that the modified layer could improve the conductivity and enhance the electrochemical signal transmission. When FA was added to modify the electrode, the electrical signal was slightly reduced to 18.23 μA (curve c). This may be due to the fact that FA blocked the electron transfer on the electrode surface, but it also demonstrated the successful modification of FA. Finally, when the cells were immobilized to the FA/RGO/MoS$_2$ modified electrode, the peak current decreased to 9.00 μA due to the insulation of the cells, which also demonstrated the success of cell immobilization (curve a).

To select an appropriate cell concentration for immobilization, a DPV measurement was performed on the RGO/MoS$_2$ modified SPCE surface to optimize the adsorption capacity of Hep G2 cells (Fig. 1 C). With increasing cell concentration, the peak current value gradually decreased, possibly because the

cells blocked the electron transfer on the electrode surface when they were immobilized on the electrode surface. Then, the increase in electrode resistance hindered the electron transfer on the electrode surface, which strongly reduced the peak current [36]. As shown in Fig. 1 D, when the cell concentration was 2×10^2 cells/mL, the maximum peak current value was 18 μA, and when the cell concentration finally increased to 2×10^8 cells/mL, the peak current value decreased to 8.7 μA. Therefore, we can determine that the peak current gradually decreased with increasing cell concentration in a certain range; however, when the number of cells increased to 2×10^6 cells/mL, the current response changed slightly and remained stable, indicating the maximum number of cells on the electrode surface. Therefore, the optimal quantity of the Hep G2 cells immobilized on the electrodes was 2×10^6 cells/mL.

Electrochemical measurement of heavy metal ions Cd^{2+}, Hg^{2+}, and Pb^{2+}

The electrochemical response of Hep G2 cells stimulated by different heavy metal ions on the surface of the modified electrode was monitored by a DPV method. Since the presence of the cells on the surface of electrodes restricts the current flow

on the electrodes because of the insulating properties of the cellular membranes and thereby increases the electrode impedance. However, heavy metal ions can cause damage to the cell membrane and lead to the outflow of intracellular substances, thus weakening the adhesion of cells on the electrode. The decrease of cell adhesion reduces the electron transfer resistance and increases the electron transfer rate on the electrode surface, which eventually leads to the decrease of cellular impedance and the increase of current value [37]. Hence, effective evaluation of target toxicity can be realized by measuring the electrochemical sensing capability of living cells. In this study, Hep G2 cells stimulated by different concentrations of heavy metal ions Cd^{2+}, Hg^{2+}, and Pb^{2+} were used for toxicity analysis through DPV measurement and are shown in Fig. 2. Significant changes in peak current of Hep G2 cells treated with different concentrations of heavy metal ions were observed. These results show that the variation trends of peak current were positively correlated with the concentration of heavy metal ions. First, as the concentration of heavy metal Cd^{2+} increased from 5 to 140 μM, the peak current value gradually increased, but when the concentration increased over 140 μM, the peak current tended to be stable. For the heavy metal mercury, there is a similar trend, for when the concentration of Hg^{2+} increased from 5 to 120 μM, the peak current gradually increased with the accumulation of heavy metal ions. However, when the concentration was

greater than 120 μM, the peak current remained stable because lead ions are less toxic in the low concentration range. Therefore, when the concentration of Pb^{2+} increased from 10 to 3000 μM, the peak current rapidly increased when the concentration was lower than 500 μM but increased slowly when the concentration was higher than 500 μM. In conclusion, these results demonstrated that the DPV peak current signals measured by the developed electrochemical cell sensor were dose-dependent with different heavy metal ions, and the measured cytotoxicity gradually increased with increasing concentrations of heavy metal ions.

Toxicity evaluation of heavy metal ions Cd^{2+}, Hg^{2+}, and Pb^{2+}

According to the formula of toxicity evaluation, the toxicity of heavy metal ions measured by the electrochemical cell sensor was accurately calculated. Meanwhile, to verify the accuracy of this cell sensor for toxicity evaluation, the electrochemical detection results were compared with the conventional MTT method.

The comparative results are shown in Fig. 3 that when the concentration of Cd^{2+} increased from 5 to 160 μM, the activity inhibition rate of Hep G2 cells increased from 7.67 to 87.67%. Similarly, when the concentration of Hg^{2+} increased from 5 to 160 μM, the activity inhibition rate of Hep G2 cells
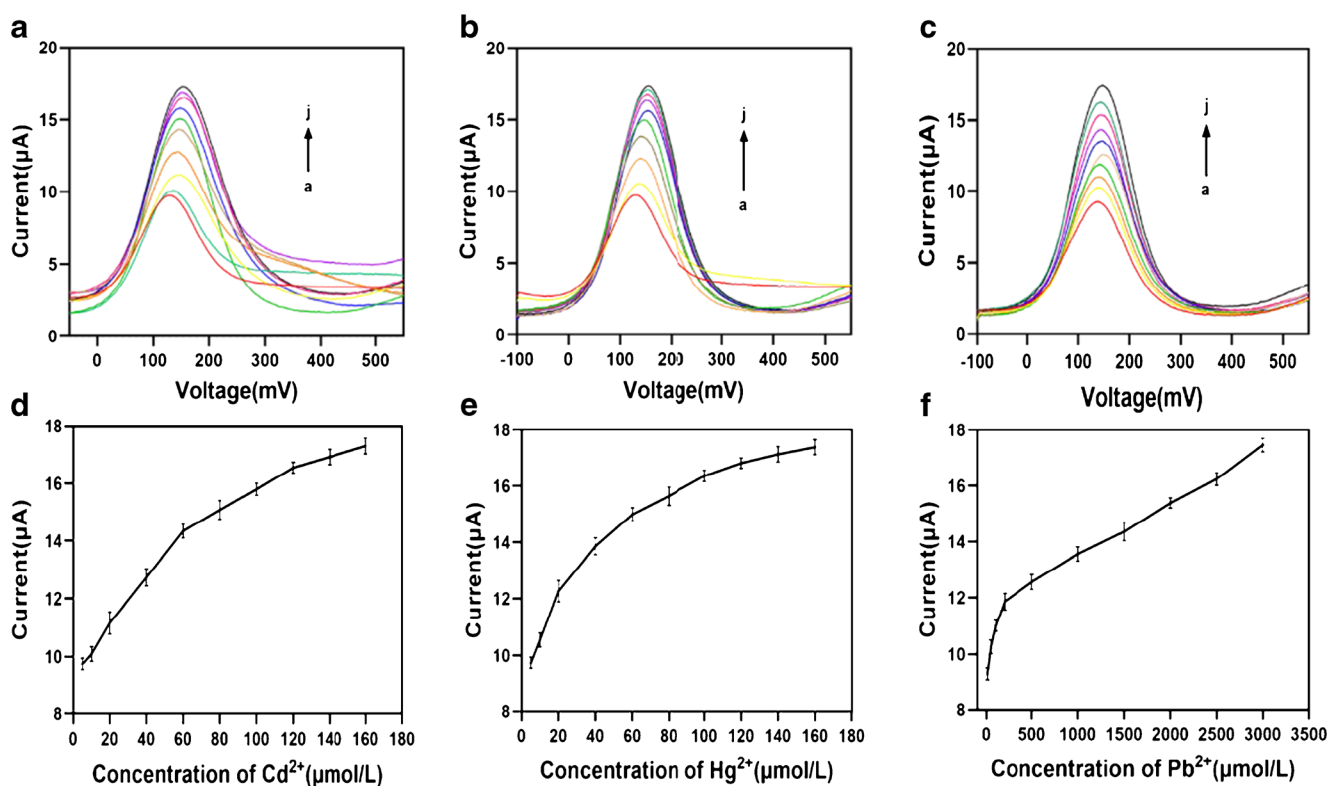

Fig. 2 Electrochemical measurement of heavy metal ions Cd^{2+}, Hg^{2+}, and Pb^{2+}. The DPV responses of cell sensor treated with different concentrations of (A) Cd^{2+}, *a* to *j*: 5 to 160 μM; (B) Hg^{2+}, *a* to *j*: 5 to 160 μM; and (C) Pb^{2+}, *a* to *j*: 10 to 3000 μM. The change of peak current value of cell sensor induced by different concentrations of (D) Cd^{2+}, (E) Hg^{2+}, and (F) Pb^{2+}
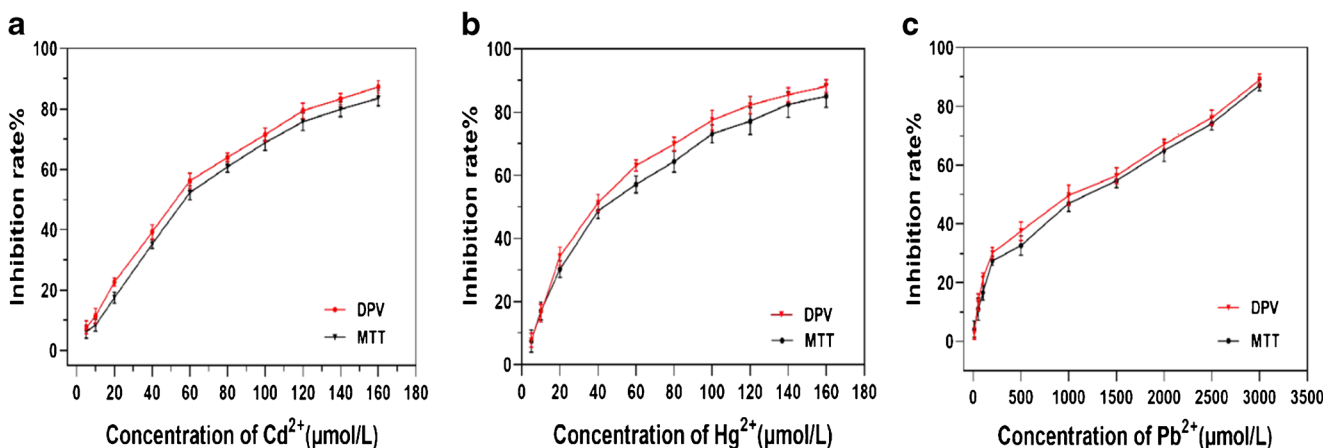
Fig. 3 Cytotoxicity curves for 6-h exposure of the Hep G2 cells on Cd^{2+}, Hg^{2+}, and Pb^{2+} obtained by using MTT assay and the proposed electrochemical method. (A) Cd^{2+}: 5, 10, 20, 40, 60, 80, 100, 120, 140, and 160 μM. (B) Hg^{2+}: 5, 10, 20, 40, 60, 80, 100, 120, 140, and 160 μM. (C) Pb^{2+}: 10, 50, 100, 200, 500, 1000, 1500, 2000, 2500, and 3000 μM

increased from 7.67 to 88.24%. However, when the concentration of Pb^{2+} increased from 10 to 3000 μM, the activity inhibition rate of Hep G2 cells increased from 2.76 to 89.03%. The calculated IC_{50} values were calculated as 49.8 μM, 36.9 μM, and 733.9 μM, for Cd^{2+}, Hg^{2+}, and Pb^{2+}, respectively. Unsurprisingly, similar results were also found in the MTT assays for when the concentration of Cd^{2+} increased from 5 to 160 μM, the activity inhibition rate of Hep G2 cells increased from 6.25 to 83.58%. When the concentration of Hg^{2+} concentration increased from 5 to 160 μM, the activity inhibition rate of Hep G2 cells increased from 7.45 to 85.05%, and when the concentration of Pb^{2+} increased from 10 to 3000 μM, the activity inhibition rate of Hep G2 cells increased from 4.13 to 87.25%. Therefore, the heavy metal ion concentration corresponding to half maximum cytotoxicity was defined as the IC_{50} value, which was calculated as 57.3 μM, 42.6 μM, and 878.1 μM for Cd^{2+}, Hg^{2+}, and Pb^{2+}, respectively.

The above experimental results showed that in the range of effective toxic dose, the toxicity of Hg^{2+} to Hep G2 cells was the highest, the toxicity of Cd^{2+} was slightly weaker, and the toxicity of Pb^{2+} was the lowest. We can also find that the results obtained by these two toxicity assessment methods have similar trends, but the electrochemical sensing method has the advantages of short detection time, simple operation, and high sensitivity. In addition, the traditional toxicity analysis experiments have also successfully verified the accuracy of the evaluation method based on electrochemical cell sensor.

To investigate the combined toxicity of heavy metal ions interacting together, different heavy metal ions with a dose concentration lower than IC_{50} were selected. The combined toxicity analysis results of two heavy metal ions or three heavy metal ions are shown in Table 1. After the cells were treated with different combinations of Cd^{2+}, Hg^{2+}, and Pb^{2+}, the CI index method was employed to determine the type of combined toxicity. The CI values can be used to quantitatively

analyze the toxicity degree of the combined action. When CI < 0.9, there are synergistic effects, 0.9 < CI < 1.1 represents an additive effect, CI > 1.1 represents an antagonistic effect, and the analytical results are all shown in Table 1. We can find that although different combinations of Cd^{2+}, Hg^{2+}, and Pb^{2+} had different toxicities to the Hep G2 cells, the total toxicity effect of the different combination groups was all enhanced with increasing doses. When Cd^{2+} and Hg^{2+} coexisted, the combined toxicity effect to Hep G2 cells was antagonistic, while when Cd^{2+} and Pb^{2+} coexist, the combined toxicity effect was synergistic, and the coexistence of Hg^{2+} and Pb^{2+} showed a synergistic effect. However, when Cd^{2+}, Hg^{2+}, and Pb^{2+} were combined together, the toxicity effect was antagonistic at low doses, but the toxicity effect to Hep G2 cells changed to the additive effect when the doses of Cd^{2+}, Hg^{2+}, and Pb^{2+} increased. Moreover, the electrochemical measurement results had the same trend as those measured by the MTT method (ESM Table S1), which proved that this study can provide a convenient new method for the evaluation of toxicity of heavy metal ions.

Cytotoxicity effects of Cd^{2+}, Hg^{2+}, and Pb^{2+} on Hep G2 cells

Conventional cytotoxicology methods were used to verify the accuracy of electrochemical measurements. As shown in the SEM images in Fig. 4 A (a), Hep G2 cells without heavy metal ion stimulation maintained their common shape and were integrated, widely diffused, and tightly attached to the surface, emitting pseudopods on the surface of the cytoplasmic membrane. However, as seen in Fig. 4 A (b, c, d), the cell morphologies of Hep G2 cells significantly changed after different heavy metal ion treatments (a: Cd^{2+}, b: Hg^{2+}, c: Pb^{2+}, respectively). In particular, the cell surface became roughened and perforated, cytoplasmic efflux occurred, cytoplasmic membrane became damaged, and apoptotic cells were separated

Table 1 Combination index (CI) values for the different heavy metal ion combinations using the proposed electrochemical method

Combination of heavy metal ions (μM)			Inhibition of viability%	CI	Indication
Cd^{2+}	Hg^{2+}	Pb^{2+}			
10	8		24.36	1.446	Antagonism
20	15		48.20	1.274	Antagonism
30	20		57.63	1.369	Antagonism
10		40	22.60	0.847	Synergism
20		100	36.75	0.891	Synergism
30		200	59.20	0.557	Synergism
	8	40	27.59	0.615	Synergism
	15	100	55.25	0.345	Synergism
	20	200	63.74	0.424	Synergism
10	8	40	28.62	1.261	Antagonism
20	15	100	48.48	1.061	Additive effect
30	20	200	64.12	0.903	Additive effect

CI < 0.9, CI = 0.9~1.1, and CI > 1.1 indicate synergism, additive effect, and antagonism, respectively

from substrates and neighboring cells. Furthermore, we investigated the cytotoxic effects of Cd^{2+}, Hg^{2+}, and Pb^{2+} on Hep G2 apoptosis using flow cytometry and fluorescence staining. Apoptosis experiments were performed to verify the accuracy and effectiveness of the cell sensing method. First, the rise of intracellular ROS levels can lead to cell membrane and DNA and mitochondrial oxidative damage, resulting in cell apoptosis. In Fig. 4 B, different levels of ROS can be visually observed in the normal cells and cells stimulated by three kinds of heavy metal ions. In Fig. 4 B (a), as the control group, there were fewer fluorescent spots in the cells, while in Fig. 4 B (b, c, d), there were a large number of intracellular fluorescent spots after being stimulated by three heavy metal ions, indicating that the intracellular ROS level increased after being stimulated by these heavy metal ions. Therefore, based on the ROS results above, it can be proven that the production of apoptosis in this study may be closely related to the ROS level. To specifically investigate the apoptosis rate and stage of apoptotic cells, an Annexinv-FITC/PI apoptosis detection kit was used to detect apoptosis by flow cytometry. The detection results are shown in Fig. 4 C and D. The proportion of normal cells in the three kinds of heavy metal ions stimulation groups was significantly decreased compared with the control group ($P < 0.01$). The proportion of normal cells in the Cd^{2+}, Hg^{2+}, and Pb^{2+} stimulation groups decreased to 59.7%, 51.6%, and 54.6%, respectively, compared with the rate of 97.3% in the control group. The proportion of early apoptosis, late apoptosis, and dead cells significantly increased in each heavy metal ions stimulation groups ($P < 0.01$). The rate of early apoptosis increased to 24.2%, 22.6%, and 7.06%, respectively, compared with the rate of 2.47% in the control group, and the rate of late apoptosis and necrosis increased

to 16.1%, 25.7%, and 38.1%, respectively, compared with the rate of 0.25% in the control group. We can see from these data that the heavy metal ion-stimulated cells can cause varying degrees of apoptosis, and early apoptosis rates were higher than late apoptosis rates in the Cd^{2+} stimulation group, while early apoptosis rates were lower than the late apoptosis rates in the Hg^{2+} and Pb^{2+} stimulation groups. This proved that the influences of different heavy metal ions on cytotoxicity were different.

Real sample evaluation

The Market-purchased rice was selected to verify the ability of the proposed cell sensor to evaluate heavy metal toxicity in real samples. After removing impurities, the rice was ground and sifted through a 40-mesh sieve. Then, 10 g of pure rice was digested by the wet digestion method. Different concentrations (low, medium, and high doses) of Cd^{2+}, Hg^{2+}, and Pb^{2+} were spiked after pretreatment of real samples. The toxicity analysis was calculated using the cytotoxicity curves in Fig. 3. Toxicity test results of rice real samples spiked with heavy metal ions are shown in ESM Table S3. No toxicity was detected in the blank group (rice spiked with no heavy metal ions); however, there was no significant difference in cytotoxicity between the sample group (rice spiked with different kinds and concentrations of heavy metal ions) and control group (DMEM spiked with different kinds and concentrations of heavy metal ions) calculated by the electrochemical cell sensor ($P > 0.05$), with good stability and accuracy. They had similar toxicity effect and owned good stability and accuracy, which proved that this cell sensor can be used to measure the toxicity of heavy metal ions in food real samples.
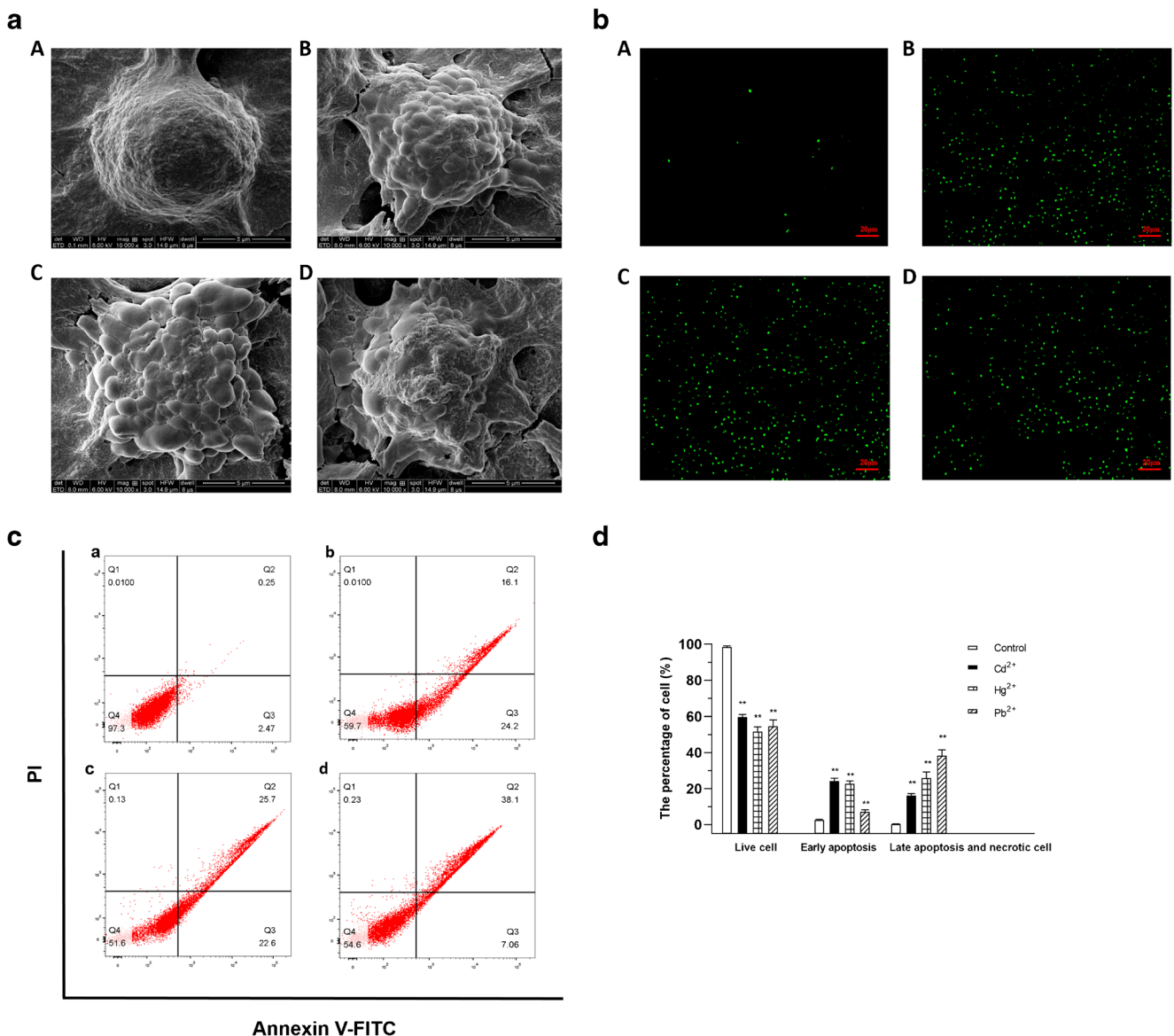
Fig. 4 Effect of heavy metal ions on the viability of Hep G2 cells. (A) The morphology of cells treated with different heavy metal ions for 6 h. (B) The fluorescence intensity of ROS in Hep G2 cells with different treatments. (C) FACS analysis of apoptosis in Hep G2 cells with different treatments. (D) The distribution of apoptosis in the different stages of Hep G2 cells. (A, B, D) a: control group, b: Cd^{2+}, c: Hg^{2+}, d: Pb^{2+}. The IC$_{50}$ value obtained by the cell sensing method was selected for the test concentration in each group. **$P < 0.01$

Conclusion and perspectives

In this study, a portable electrochemical Hep G2 cell sensor based on a smartphone was developed to evaluate the toxicity of different heavy metal ions. Our results showed that Cd^{2+}, Hg^{2+}, and Pb^{2+} induced a significant decrease in the cell viability in a dose-dependent manner. Differential pulse voltammetry spectroscopy values decreased with concentrations of Cd^{2+}, Hg^{2+}, and Pb^{2+} in the range of 5 to 160 μM, 5 to 160 μM, and 10 to 3000 μM, respectively. The IC$_{50}$ values for Cd^{2+}, Hg^{2+}, and Pb^{2+} were calculated as 49.83 μM, 36.94 μM, and 733.90 μM, respectively, by the electrochemical method, and 57.26 μM, 42.60 μM, and 878.1 μM, respectively, by the MTT assay. A synergistic effect was observed between Cd^{2+} and Pb^{2+} and between Hg^{2+}and Pb^{2+}. Binary mixtures of Cd^{2+} and Hg^{2+} revealed an antagonistic effect. Ternary mixtures of Cd^{2+}, Hg^{2+}, and Pb^{2+} also showed an antagonistic effect at low doses but achieved an additive effect at high doses. These results were confirmed by conventional cytotoxicology experiments which proved that the developed electrochemical cell sensing method can effectively and accurately monitor the whole process of cell apoptosis induced by different heavy metal ion stimulation and can be developed as a convenient and effective tool to investigate mycotoxin toxicity.

Recently, non-targeted screening technology is gradually becoming an effective way to promote food safety monitoring from passive detection to active prevention. Although the cell sensing method developed in this study cannot distinguish unknown heavy metal ions, it is easy to accurately identify and evaluate different toxic heavy metal ions by comparing their electrochemical characteristic spectra if a large toxicity database of different heavy metal ions is established in advance.

Declarations

Conflict of interest The authors declare no competing interests.

References

1. Lu Y, Liang X, Niyungeko C, Zhou J, Xu J, Tian G. A review of the identification and detection of heavy metal ions in the environment by voltammetry. Talanta. 2018;178:324–38.

2. Kim J-J, Kim Y-S, Kumar V. Heavy metal toxicity: an update of chelating therapeutic strategies. J Trace Elem Med Biol. 2019;54: 226–31.

3. Rebelo FM, Caldas ED. Arsenic, lead, mercury and cadmium: toxicity, levels in breast milk and the risks for breastfed infants. Environ Res. 2016;151:671–88.

4. Hamida S, Ouabdesslam L, Ladjel A, Escudero M, Anzano J. Determination of cadmium, copper, lead, and zinc in pilchard sardines from the Bay of Boumerdés by atomic absorption spectrometry. Anal Lett. 2018;51(16):2501–8.

5. Ramdani S, Amar A, Belhsaien K, El Hajjaji S, Ghalem S, Zouahri A, et al. Assessment of heavy metal pollution and ecological risk of roadside soils in Tlemcen (Algeria) using flame-atomic absorption spectrometry. Anal Lett. 2018;51(15):2468–87.

6. Jaswal BBS, Rai PK, Singh T, Zorba V, Singh VK. Detection and quantification of heavy metal elements in gallstones using X-ray fluorescence spectrometry. Xray Spectrom. 2019;48(3):178–87.

7. Mohamed R, Zainudin BH, Yaakob AS. Method validation and determination of heavy metals in cocoa beans and cocoa products by microwave assisted digestion technique with inductively coupled plasma mass spectrometry. Food Chem. 2020;303:125392.

8. Wang L, Peng X, Fu H, Huang C, Li Y, Liu Z. Recent advances in the development of electrochemical aptasensors for detection of heavy metals in food. Biosens Bioelectron. 2020;147:111777.

9. Cui Z, Luan X, Jiang H, Li Q, Xu G, Sun C, et al. Application of a bacterial whole cell biosensor for the rapid detection of cytotoxicity in heavy metal contaminated seawater. Chemosphere. 2018;200: 322–9.

10. Lauri A, Soliman D, Omar M, Stelzl A, Ntziachristos V, Westmeyer GG. Whole-cell photoacoustic sensor based on pigment relocalization. ACS Sens. 2019;4(3):603–12.

11. Gupta N, Renugopalakrishnan V, Liepmann D, Paulmurugan R, Malhotra BD. Cell-based biosensors: recent trends, challenges and future perspectives. Biosens Bioelectron. 2019;141:111435.

12. Jeon H, Lee E, Kim D, Lee M, Ryu J, Kang C, et al. Cell-based biosensors based on intein-mediated protein engineering for detection of biologically active signaling molecules. Anal Chem. 2018;90(16):9779–86.

13. Jiang D, Ge P, Wang L, Jiang H, Yang M, Yuan L, et al. A novel electrochemical mast cell-based paper biosensor for the rapid detection of milk allergen casein. Biosens Bioelectron. 2019;130: 299–306.

14. Jiang D, Liu Y, Jiang H, Rao S, Fang W, Wu M, et al. A novel screen-printed mast cell-based electrochemical sensor for detecting spoilage bacterial quorum signaling molecules (N-acyl-homoserine-lactones) in freshwater fish. Biosens Bioelectron. 2018;102:396–402.

15. Cardoso RM, Kalinke C, Rocha RG, Dos Santos PL, Rocha DP, Oliveira PR, et al. Additive-manufactured (3D-printed) electrochemical sensors: a critical review. Anal Chim Acta. 2020;1118: 73–91.

16. Shin J, Kim S, Yoon T, Joo C, Jung H-I. Smart Fatigue Phone: real-time estimation of driver fatigue using smartphone-based cortisol detection. Biosens Bioelectron. 2019;136:106–11.

17. Deng W, Dou Y, Song P, Xu H, Aldalbahi A, Chen N, et al. Lab on smartphone with interfaced electrochemical chips for on-site gender verification. J Electroanal Chem. 2016;777:117–22.

18. Morais S, Tortajada-Genaro LA, Maquieira Á, Gonzalez Martinez M-Á. Biosensors for food allergy detection according to specific IgE levels in serum. Trends Anal Chem. 2020;127.

19. Minnetti E, Chiariotti P, Paone N, Garcia G, Vicente H, Violini L, et al. A smartphone integrated hand-held gap and flush measurement system for in line quality control of car body assembly. Sensors. 2020;20(11):3300.

20. Lu L, Jiang Z, Hu Y, Zhou H, Liu G, Chen Y, et al. A portable optical fiber SPR temperature sensor based on a smart-phone. Opt Express. 2019;27(18):25420–7.

21. Jiang D, Zhu P, Jiang H, Ji J, Sun X, Gu W, et al. Fluorescent magnetic bead-based mast cell biosensor for electrochemical detection of allergens in foodstuffs. Biosens Bioelectron. 2015;70:482–90.

22. Ramaraj S, Sakthivel M, Chen S-M, Elshikh MS, Chen T-W, Yu M-C, et al. Electrochemical sensing of anti-inflammatory agent in paramedical sample based on FeMoSe₂ modified SPCE: comparison of various preparation methods and morphological effects. Anal Chim Acta. 2019;1083:88–100.

23. Yin S, Li C, Wang S, Ren X, Zeng L, Zhang L. The construction of a 2D MoS₂-based binder-free electrode with a honeycomb structure for enhanced electrochemical performance. Dalton Trans. 2020;49(24):8036–40.

24. Mazaheri A, Lee M, Van Der Zant HS, Frisenda R, Castellanos-Gomez A. MoS₂-on-paper optoelectronics: drawing photodetectors with van der Waals semiconductors beyond graphite. Nanoscale. 2020;12(37):19068–74.

25. Ye Y, Guo H, Sun X. Recent progress on cell-based biosensors for analysis of food safety and quality control. Biosens Bioelectron. 2019;126:389–404.

26. Xiao P, Mao J, Ding K, Luo W, Hu W, Zhang X, et al. Solution-processed 3D RGO–MoS₂/pyramid Si heterojunction for ultrahigh detectivity and ultra-broadband photodetection. Adv Mater. 2018;30(31):1801729.

27. Geleta GS, Zhao Z, Wang Z. A novel reduced graphene oxide/molybdenum disulfide/polyaniline nanocomposite-based

electrochemical aptasensor for detection of aflatoxin B 1. Analyst. 2018;143(7):1644–9.

28. Qi H, Yue S, Bi S, Ding C, Song W. Isothermal exponential amplification techniques: from basic principles to applications in electrochemical biosensors. Biosens Bioelectron. 2018;110:207–17.

29. Law S, Leung AW, Xu C. Folic acid-modified celastrol nanoparticles: synthesis, characterization, anticancer activity in 2D and 3D breast cancer models. Artif Cells Nanomed Biotechnol. 2020;48(1): 542–59.

30. Gu W, Zhu P, Jiang D, He X, Li Y, Ji J, et al. A novel and simple cell-based electrochemical impedance biosensor for evaluating the combined toxicity of DON and ZEN. Biosens Bioelectron. 2015;70:447–54.

31. Liu Q, Xu S, Niu C, Li M, He D, Lu Z, et al. Distinguish cancer cells based on targeting turn-on fluorescence imaging by folate functionalized green emitting carbon dots. Biosens Bioelectron. 2015;64:119–25.

32. Zhang Y, Liu J-M, Yan X-P. Self-assembly of folate onto polyethyleneimine-coated CdS/ZnS quantum dots for targeted turn-on fluorescence imaging of folate receptor overexpressed cancer cells. Anal Chem. 2013;85(1):228–34.

33. Xia S, Zhu P, Pi F, Zhang Y, Li Y, Wang J, et al. Development of a simple and convenient cell-based electrochemical biosensor for evaluating the individual and combined toxicity of DON, ZEN, and AFB1. Biosens Bioelectron. 2017;97:345–51.

34. Chen C, Wang Y, Zhao X, Qian Y, Wang Q. Combined toxicity of butachlor, atrazine and λ-cyhalothrin on the earthworm Eisenia fetida by combination index (CI)-isobologram method. Chemosphere. 2014;112:393–401.

35. Wang Y, Ni Y. Molybdenum disulfide quantum dots as a photoluminescence sensing platform for 2, 4, 6-trinitrophenol detection. Anal Chem. 2014;86(15):7463–70.

36. Jiang H, Yang J, Wan K, Jiang D, Jin C. Miniaturized paper-supported 3D cell-based electrochemical sensor for bacterial lipopolysaccharide detection. ACS Sens. 2020;5(5):1325–35.

37. Wang X, Zhu P, Pi F, Jiang H, Shao J, Zhang Y, et al. A sensitive and simple macrophage-based electrochemical biosensor for evaluating lipopolysaccharide cytotoxicity of pathogenic bacteria. Biosens Bioelectron. 2016;81:349–57.